arXiv:nucl-th/0702044v2 4 Apr 2007

Neutrino Breakup of $A = 3$ Nuclei in Supernovae

E. O'Connor,[1, 2, *] D. Gazit,[3, †] C.J. Horowitz,[4, ‡] A. Schwenk,[1, §] and N. Barnea[3, ¶]
[1] *TRIUMF, 4004 Wesbrook Mall, Vancouver, BC, Canada, V6T 2A3*
[2] *Department of Physics, UPEI, 550 University Ave, Charlottetown, PE, Canada, C1A 4P3*
[3] *Racah Institute of Physics, Hebrew University, 91904, Jerusalem, Israel*
[4] *Nuclear Theory Center and Department of Physics, Indiana University, Bloomington, IN 47408*

We extend the virial equation of state to include ^{3}H and ^{3}He nuclei, and predict significant mass-three fractions near the neutrinosphere in supernovae. While alpha particles are often more abundant, we demonstrate that energy transfer cross-sections for muon and tau neutrinos at low densities are dominated by breakup of the loosely-bound ^{3}H and ^{3}He nuclei. The virial coefficients involving $A = 3$ nuclei are calculated directly from the corresponding nucleon-^{3}H and nucleon-^{3}He scattering phase shifts. For the neutral-current inelastic cross-sections and the energy transfer cross sections, we perform ab-initio calculations based on microscopic two- and three-nucleon interactions and meson-exchange currents.

PACS numbers: 26.50.+x, 25.30.Pt, 21.65.+f, 97.60.Bw
Keywords: Low-density nuclear matter, neutrino scattering, supernovae

I. INTRODUCTION

Core-collapse supernovae (SN) are giant explosions of massive stars that radiate 99% of their energy in neutrinos. Therefore, the dynamics and the neutrino signals can be sensitive to the details of neutrino interactions with nucleonic matter. At present, most SN simulations with detailed neutrino microphysics do not explode, but they may be close to successful explosions (for a status report, see [1, 2]). Supernovae radiate electron, muon and tau neutrinos. Electron neutrinos can exchange energy with matter via charged-current interactions. Energy transfer from muon or tau neutrinos, hereafter ν_x, is more difficult [3] because neutrino-electron scattering has a small cross section, and neutrino-nucleon elastic scattering involves only a small energy transfer.

Haxton and Bruenn proposed that ν_x can exchange energy via inelastic excitations of ^{4}He and heavier nuclei [4], whereas Hannestad and Raffelt investigated the exchange of energy between ν_x and two interacting nucleons $\nu_x\mathrm{NN} \to \nu_x\mathrm{NN}$ [5]. Recently, Juodagalvis *et al.* have calculated detailed ν_x neutral-current cross-sections for $A = 50 - 65$ nuclei [6], and Gazit and Barnea have presented microscopic results for ^{4}He cross sections [7, 8]. These inelastic excitations can aid the transfer of neutrino energy to the SN shock and can keep ν_x in thermal equilibrium to lower densities, resulting in the radiation of a lower energy ν_x spectrum [9]. First studies on the role of ^{4}He excitation for the shock revival were carried out by Ohnishi *et al.* [10].

To evaluate the role of ν_x inelastic scattering one needs both cross sections and detailed information on the composition and other thermodynamic properties of nucleonic matter. Models that describe the system with only a single average nuclear species may miss the contribution of less abundant nuclei with large cross sections. Moreover, there are many fundamental connections between the equation of state and neutrino interactions.

Nuclear statistical equilibrium (NSE) models predict abundances based on binding energies and the quantum numbers of nuclei. However, NSE models only treat approximately (or neglect) strong interactions between nuclei, and consequently break down as the density increases. We have recently developed a description of low-density nuclear matter (composed of neutrons, protons and alpha particles) in thermal equilibrium based on the virial expansion [11, 12]. The virial equation of state systematically takes into account contributions from bound nuclei and the scattering continuum, and thus provides a framework to include strong-interaction corrections to NSE models. The virial equation of state makes model-independent predictions for the conditions [13] near the neutrinosphere, for low densities $\rho \sim 10^{11-12}\,\mathrm{g/cm}^3$ and high temperatures $T \sim 4\,\mathrm{MeV}$. In particular, the resulting alpha particle concentration differs from all equations of state currently used in SN simulations, and the predicted large symmetry energy at low densities has been confirmed in near Fermi-energy heavy-ion collisions [14]. In addition, the long-wavelength neutrino response of low-density matter can be calculated consistently from the virial expansion [15].

In this paper, we extend the virial expansion to include ^{3}H and ^{3}He nuclei, and predict that the mass-three fraction can be significant (up to 10%) near the neutrinosphere. The second virial coefficients involving $A = 3$ nuclei are calculated directly from the corresponding nucleon-^{3}H and nucleon-^{3}He scattering phase shifts. While alpha particles are often more abundant due to the large binding energy ($E_4 = 28.3\,\mathrm{MeV}$ compared to $E_3 \sim 8\,\mathrm{MeV}$), we show that mass-three nuclei are important

---

[*] E-mail: evanoc@triumf.ca
[†] E-mail: gdoron@phys.huji.ac.il
[‡] E-mail: horowit@indiana.edu
[§] E-mail: schwenk@triumf.ca
[¶] E-mail: nir@phys.huji.ac.il

for energy transfer, in particular for the more energetic muon and tau neutrinos with $E_{\nu_x} \sim 20\,\mathrm{MeV}$. For neutrinos with these energies, we find that the neutral-current inelastic energy transfer cross-sections and the neutrino energy loss for $T \gtrsim 4\,\mathrm{MeV}$ are dominated by the breakup of the loosely-bound ^{3}H and ^{3}He nuclei. Our predictions for the neutral-current inclusive inelastic cross-sections on mass-three nuclei are based on microscopic two- and three-nucleon interactions and meson-exchange currents, and include full final-state interactions via the Lorentz integral transform (LIT) method [16].

This paper is organized as follows. In Section II, we generalize the virial equation of state to include $A = 3$ nuclei, and present results for the composition of low-density nuclear matter for various temperatures, densities and proton fractions. In Section III A, we calculate the inelastic ^{3}H and ^{3}He neutral-current cross-sections and energy transfer cross-sections. We combine our results in Section III B and study the neutrino energy loss for conditions near the neutrinosphere. Finally, we conclude in Section IV.

II. COMPOSITION OF LOW-DENSITY NUCLEAR MATTER

In this section, we discuss the virial equation of state and present results for the composition of low-density nuclear matter including $A = 3$ nuclei (for details and additional thermodynamic results, see [17]).

To determine the abundance of $A = 3$ nuclei near the neutrinosphere in supernovae, we extend the virial approach of Refs. [11, 12] to include ^{3}H and ^{3}He nuclei. In the corresponding virial expansion, neutrons, protons, α particles, ^{3}H and ^{3}He nuclei are explicitly included, deuterons are included as a bound state contribution to the proton-neutron virial coefficient. We will explicitly consider deuterons and neutrino-deuteron scattering in future work. The equation of state is determined through an expansion of the pressure P in the fugacities (see for instance [18]) up to second order,

$$
\begin{aligned}
\frac{P}{T} = {} & \frac{2}{\lambda_{\mathrm{N}}^3}\big(z_n + z_p + (z_n^2 + z_p^2)\, b_n + 2 z_n z_p\, b_{pn}\big) \\
& + \frac{1}{\lambda_\alpha^3}\big(z_\alpha + z_\alpha^2\, b_\alpha + 2 z_\alpha (z_n + z_p)\, b_{\alpha n}\big) \\
& + \frac{2}{\lambda_{^3\mathrm{He}}^3}\big(z_{^3\mathrm{He}} + 2 z_{^3\mathrm{He}}(z_p\, b_{p^3\mathrm{He}} + z_n\, b_{n^3\mathrm{He}})\big) \\
& + \frac{2}{\lambda_{^3\mathrm{H}}^3}\big(z_{^3\mathrm{H}} + 2 z_{^3\mathrm{H}}(z_p\, b_{p^3\mathrm{H}} + z_n\, b_{n^3\mathrm{H}})\big)\,, \qquad (1)
\end{aligned}
$$

where T is the temperature, $z_i = e^{(\mu_i + E_i)/T}$ is the fugacity (with chemical potential μ_i and binding energy E_i), $\lambda_i = \sqrt{2\pi/m_i T}$ is the thermal wavelength of particle i, and b_{ij} are the second virial coefficients describing interactions between particles i, j ($b_i \equiv b_{ii}$). We have calculated these virial coefficients from phases shifts and low-energy scattering lengths, see Ref. [17] for details. The second virial coefficients b_n, b_{pn}, b_α and $b_{\alpha n}$ are tabulated in [11], and the additional virial coefficients involving $A = 3$ nuclei are given in Table I from $T = 1\,\mathrm{MeV}$ to $10\,\mathrm{MeV}$. Due to a lack of p-^{3}H scattering data, we assume that $b_{p^3\mathrm{H}} \approx b_{n^3\mathrm{He}}$. The effects of interactions with $A = 3$ nuclei are expected to be small at low densities (see also the hierarchy observed in Ref. [11]) and therefore we neglect $b_{^3\mathrm{He}^3\mathrm{He}}$, $b_{^3\mathrm{H}^3\mathrm{H}}$, $b_{^3\mathrm{He}^3\mathrm{H}}$, $b_{\alpha^3\mathrm{He}}$ and $b_{\alpha^3\mathrm{H}}$.

T [MeV]	$b_{p^3\mathrm{He}}$	$b_{n^3\mathrm{H}}$	$b_{n^3\mathrm{He}}$
1	0.043	-0.002	-0.244
2	0.245	0.253	-0.067
3	0.407	0.429	0.045
4	0.528	0.555	0.113
5	0.617	0.645	0.153
6	0.680	0.708	0.176
7	0.725	0.751	0.189
8	0.754	0.778	0.195
9	0.772	0.795	0.198
10	0.781	0.803	0.198

TABLE I: Nucleon-^{3}H and nucleon-^{3}He virial coefficients for temperatures of $T = 1\,\mathrm{MeV}$ to $10\,\mathrm{MeV}$.

The particle densities can be obtained by partial derivatives of the pressure with respect to the corresponding fugacities,

$$
n_i = z_i \left(\frac{\partial}{\partial z_i}\frac{P}{T}\right)_T . \qquad (2)
$$

By assuming chemical equilibrium,

$$
\mu_\alpha = 2\mu_n + 2\mu_p\,, \qquad (3)
$$

$$
\mu_{^3\mathrm{H}} = 2\mu_n + \mu_p\,, \qquad (4)
$$

$$
\mu_{^3\mathrm{He}} = \mu_n + 2\mu_p\,, \qquad (5)
$$

the corresponding $A = 3, 4$ fugacities are determined by the proton and neutron fugacities and the corresponding binding energy: $z_{^3\mathrm{H}} = z_n^2 z_p e^{E_{^3\mathrm{H}}/T}$ for example. For a given baryon density n_b and proton fraction Y_p, the fugacities z_p and z_n are then determined implicitly from

$$
n_b = n_p + n_n + 4n_\alpha + 3n_{^3\mathrm{He}} + 3n_{^3\mathrm{H}}\,, \qquad (6)
$$

$$
Y_p = (n_p + 2n_\alpha + 2n_{^3\mathrm{He}} + n_{^3\mathrm{H}})/n_b\,. \qquad (7)
$$

The resulting mass fractions ($x_i = A_i n_i / n_b$) are shown in Fig. 1 for neutrinosphere densities and temperatures, and various proton fractions.

For a density of $10^{12}\,\mathrm{g/cm^3}$, we find that the total mass-three fraction is significant, up to $x_{^3\mathrm{H}} + x_{^3\mathrm{He}} \approx 0.1$ in symmetric matter. Moreover, for temperatures $T \gtrsim 5\,\mathrm{MeV}$ (and increasingly important at low proton fractions), the ^{3}H mass fraction is larger than the α particle

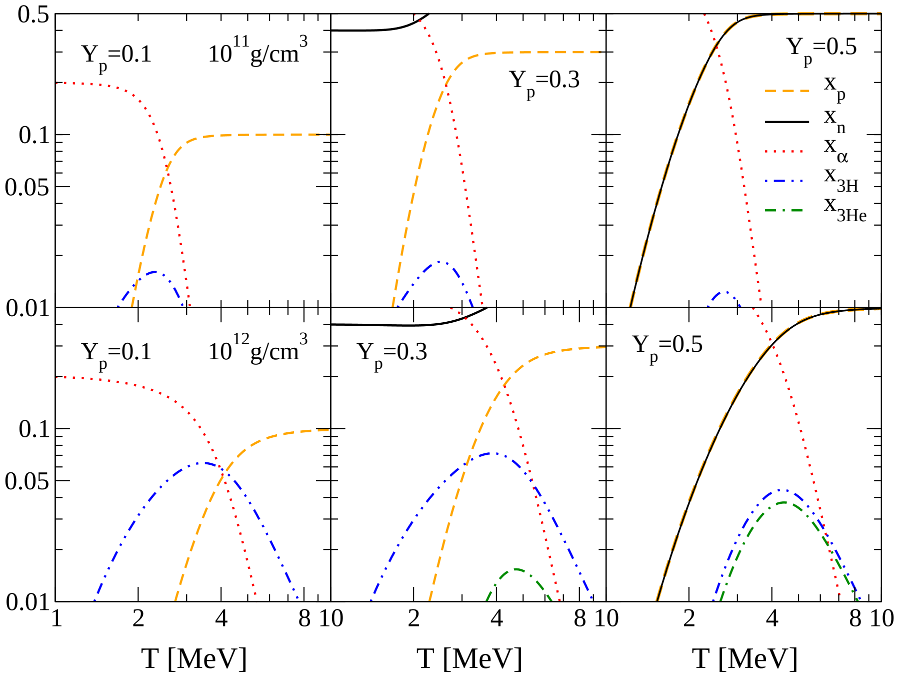

FIG. 1: (Color online) Mass fractions of nucleons and $A = 3, 4$ nuclei in chemical equilibrium as a function of temperature T. The top and bottom rows correspond to a density of 10^{11} g/cm^3 and 10^{12} g/cm^3 respectively, and from left to right the proton fractions are $Y_p = 0.1, 0.3$ and 0.5. For this temperature range, at 10^{11} g/cm^3 the neutron fugacity is $z_n < 0.1, 0.05, 0.01$ for $Y_p = 0.1, 0.3$ and 0.5 respectively, all other fugacities are < 0.01 for all shown proton fractions. At the higher density, 10^{12} g/cm^3, the neutron fugacity is $z_n < 0.7, 0.35, 0.04$ for $Y_p = 0.1, 0.3$ and 0.5 respectively, all other fugacities are < 0.06 for all shown proton fractions.

fraction. We also observe that at lower temperatures, where many of the protons are bound in alpha particles (and heavy nuclei), ^{3}H nuclei are more abundant than free protons. Here, the rate of electron capture may be dominated by capture on ^{3}H, since the capture on ^{4}He has low cross sections and there are few free protons. The contribution of mass-three nuclei to charged-current interactions will be left to future work [19]. Finally, we emphasize that heavier nuclei and larger clusters become important as the α particle fraction saturates at very low temperature.

III. NEUTRINO-^{3}H AND -^{3}He BREAKUP: NEUTRAL-CURRENT CROSS-SECTIONS

The calculation of the neutral-current inclusive inelastic cross-sections on ^{3}H and ^{3}He follows Ref. [8]. We solve the three-nucleon problem based on the Argonne v_{18} nucleon-nucleon [20] and the Urbana IX three-nucleon [21] interactions. Neutrino scattering on $A = 3$ nuclei only induces transitions to continuum states, since ^{3}H and ^{3}He have no excited states. Hence, a correct description must include breakup channels and final-state interactions among the three nucleons. We include these via the LIT method [16], which uses an integral transform with a lorentzian kernel to reduce the continuum problem to a bound-state-like problem. The resulting Schrödinger-like equations are solved using the effective interaction hyperspherical harmonics (EIHH) approach [22, 23]. The combination of these approaches converges rapidly and yields a numerical precision of less than a percent for few-body reaction cross-sections [7, 8, 24, 25]. The energy transfer due to elastic scattering is low, $\omega \sim T^2/m$, and therefore we include only breakup channels in our calculations.

Since the energy scale of SN neutrinos is much smaller than the mass of the Z-boson, the neutrino-nucleus interaction can be approximated by an effective current-current Hamiltonian. The neutrino current is straightforward and results in kinematical factors to the cross section. The standard model dictates only the formal structure of the nuclear neutral-current:

$$J^0_\mu = (1 - 2\sin^2\theta_W)\,\frac{\tau_0}{2}\,J^V_\mu + \frac{\tau_0}{2}\,J^A_\mu - \sin^2\theta_W\,J^V_\mu\,, \qquad (8)$$

where the superscripts A, V denote axial and vector currents. For supernova neutrinos, chiral effective field theory (EFT) of nucleons and pions offers a consistent approach to nuclear interactions and electro-weak currents. For historical reasons, the present calculation uses conventional two- and three-nucleon interactions and EFT currents, but future applications can be fully based on chiral EFT. The current approach has been applied to study electro-weak reactions on $A = 2, 3, 4$ nuclei [8, 26].

We use chiral EFT meson-exchange currents (MEC) at next-to-next-to-next-to-leading order. The MEC are based on a momentum expansion in Q/Λ, where $Q \sim 10-20\,\text{MeV}$ is the typical energy in our process of interest, and the cutoff Λ is of the order of the EFT breakdown scale. Here, we follow Park *et al.* [26] and vary the cutoff over the range $\Lambda = 400-800\,\text{MeV}$. In configuration space, the MEC are obtained from a Fourier transform of propagators with a cutoff Λ. This leads to a cutoff dependence, which is renormalized by a cutoff-dependent counterterm. In the present case, all other low-energy coefficients can be determined from pion-nucleon scattering. The counterterm $d_r(\Lambda)$ characterizes the strength of a two-nucleon contact operator and has been matched to the triton half-life over this cutoff range. As a check, we reproduce the cutoff dependence $d_r(\Lambda)$ of Ref. [26].

A. Inelastic cross-sections and energy transfer

The calculated cross sections are averaged over energy and angle, assuming a Fermi-Dirac distribution for the neutrinos with zero chemical potential, temperature T_ν, and neutrino momentum k,

$$f(T_\nu, k) = \frac{N}{{T_\nu}^3} \frac{k^2}{e^{k/T_\nu}+1} \,, \tag{9}$$

where $N^{-1} = 2\sum_{n=1}^{\infty}(-1)^{n+1}/n^3$ is a normalization factor. The quantities of interest are the temperature-averaged cross-sections and energy transfer cross-sections:

$$\langle\sigma\rangle_{T_\nu} = \int_{\omega_{\text{th}}}^{\infty} d\omega \int dk_i \, f(T_\nu, k_i) \, \frac{d\sigma}{dk_f} \,, \tag{10}$$

$$\langle\omega\sigma\rangle_{T_\nu} = \int_{\omega_{\text{th}}}^{\infty} d\omega \int dk_i \, f(T_\nu, k_i) \, \omega \, \frac{d\sigma}{dk_f} \,, \tag{11}$$

where $k_{i,f}$ are the initial and final neutrino energy, $\omega = k_i - k_f$ is the energy transfer, and ω_{th} denotes the threshold energy of the breakup reaction. In Table II, we present results for the averaged neutrino and anti-neutrino neutral-current inclusive inelastic cross-sections and energy transfer cross-sections as a function of the neutrino temperature. The difference between the ^{3}H and the ^{3}He cross sections reflects the difference in thresholds between the two nuclei. The mirror symmetry between both nuclei is restored with higher neutrino energy. The leading contributions to the cross section are the axial E_1^A, M_1^A and E_2^A multipoles. The relative importance of these multipoles varies as a function of the momentum transfer, and thus as a function of the neutrino temperature. In comparison to inelastic excitations of ^{4}He studied in Ref. [8], we find that the cross sections are about a factor 20 and 10 times larger at temperatures 4 MeV and 6 MeV respectively (for the mean values of ^{3}H and ^{3}He), and the energy transfer cross-sections are 8 and 2 times larger.

T_ν [MeV]	^{3}H		^{3}He	
1	1.97×10^{-6}	1.68×10^{-5}	3.49×10^{-6}	2.76×10^{-5}
2	4.62×10^{-4}	4.73×10^{-3}	6.15×10^{-4}	5.94×10^{-3}
3	5.53×10^{-3}	6.38×10^{-2}	6.77×10^{-3}	7.41×10^{-2}
4	2.68×10^{-2}	3.37×10^{-1}	3.14×10^{-2}	3.77×10^{-1}
5	8.48×10^{-2}	1.14	9.70×10^{-2}	1.25
6	2.09×10^{-1}	2.99	2.35×10^{-1}	3.21
7	4.38×10^{-1}	6.61	4.87×10^{-1}	7.03
8	8.20×10^{-1}	13.0	9.03×10^{-1}	13.7
9	1.41	23.4	1.54	24.6
10	2.27	39.3	2.47	41.2

TABLE II: Averaged neutrino- and anti-neutrino-^{3}H and -^{3}He neutral-current inclusive inelastic cross-sections per nucleon (A=3), $\langle\sigma\rangle_{T_\nu} = \frac{1}{2A}\,\langle\,\sigma_\nu + \sigma_{\overline{\nu}}\rangle_{T_\nu}$ (left columns), and energy transfer cross-sections, $\langle\omega\sigma\rangle_{T_\nu} = \frac{1}{2A}\,\langle\,\omega\sigma_\nu + \omega\sigma_{\overline{\nu}}\rangle_{T_\nu}$ (right columns), as a function of neutrino temperature T_ν, in units of $10^{-42}\,\text{cm}^2$ and $10^{-42}\,\text{MeVcm}^2$ respectively.

At low-momentum transfer, the Gamow-Teller operator dominates for the cross section, consequently the MEC have a large effect of about 16% at a temperature of 1 MeV. At higher-momentum transfer, higher-order multipoles start to play an important role. Due to spatial symmetry, the MEC contribution to these multipoles is small and the overall effect of MEC decreases rapidly to $< 2\%$ for temperatures above 4 MeV. While not directly important here, the asymmetry between the scattering of neutrinos and anti-neutrinos increases with temperature: The difference in the energy transfer grows gradually from 3% for a neutrino temperature of 3 MeV to $> 50\%$ for 10 MeV temperatures. Finally, the cutoff dependence of these observables is $< 2\%$ for 1 MeV and $< 1\%$ for higher temperatures. This validates our calculations. We thus estimate the precision of the predicted cross sections to be a few percent, which also includes estimates of the numerical accuracy.

B. Neutrino energy loss due to inelastic scattering

We can combine the energy transfer cross-sections with the $A = 3, 4$ mass fractions of Section II to calculate the neutrino energy loss due to inelastic excitations of $A = 3, 4$ nuclei. The neutral-current cross-sections on ^{4}He are taken from Ref. [8], which is based on the same microscopic input. A neutrino of energy E_ν will lose energy to inelastic excitations, and heat the matter, at a rate dE_ν/dx given by

$$\frac{dE_\nu}{dx} = n_b \sum_{i={}^3\text{H},\,{}^3\text{He},\,{}^4\text{He}} x_i \, \langle\omega\sigma\rangle_{i,\,T_\nu} \,. \tag{12}$$

To explore the effect of mass-three nuclei on the energy loss, we assume the neutrino energies are characterized

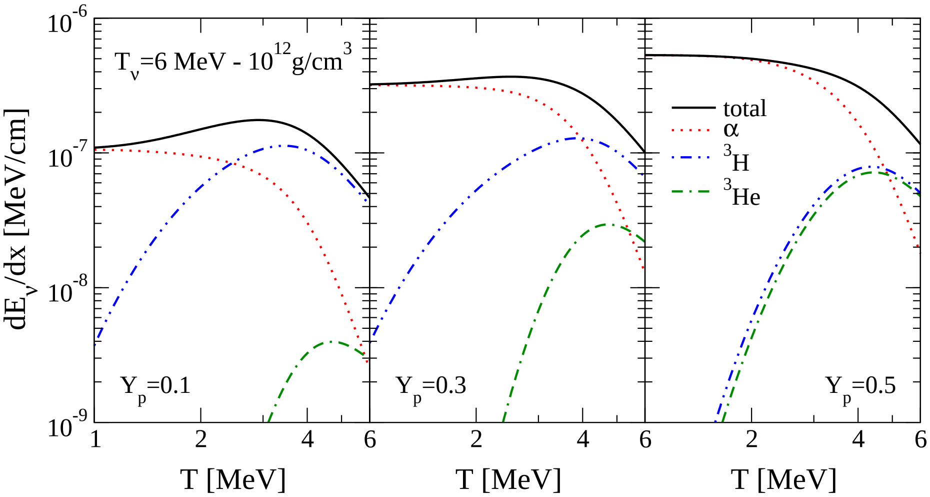

FIG. 2: (Color online) Neutrino energy loss dE_ν/dx for inelastic excitations of $A = 3, 4$ nuclei as a function of the matter temperature T at a density of $10^{12}\,\mathrm{g/cm^3}$. We assume that the the neutrino energies are characterized by a Fermi-Dirac distribution with a temperature $T_\nu = 6\,\mathrm{MeV}$. The contributions from ^{3}H, ^{3}He and ^{4}He nuclei, and the total neutrino energy loss are shown for proton fractions $Y_p = 0.1, 0.3$ and 0.5.

by a Fermi-Dirac spectrum of temperature T_ν, while the low-density matter may have a lower temperature T. For simplicity, we neglect the energy transfer from nuclei to neutrinos required by detailed balance. This is strictly correct only in the limit $T \ll T_\nu$.

In Fig. 2, the neutrino energy loss due to inelastic scattering is shown for a density of $10^{12}\,\mathrm{g/cm^3}$ and neutrino temperature $T_\nu = 6\,\mathrm{MeV}$, as a function of the matter temperature for various proton fractions. For $T \gtrsim 4\,\mathrm{MeV}$, the energy loss is dominated by the contributions from ^{3}H nuclei. The total abundance of $A = 3$ nuclei depends only weakly on the proton fraction (see Fig. 1), which is reflected in the weak dependence of the neutrino energy loss as a function of proton fraction. Finally, for lower densities, mass-three nuclei are less abundant (see Fig. 1), and therefore also their contributions to the neutrino energy loss.

IV. CONCLUSIONS

The virial expansion provides a systematic approach to low-density nuclear matter in thermal equilibrium, in particular for the conditions near the neutrinosphere with densities $\rho \sim 10^{11-12}\,\mathrm{g/cm^3}$ and temperatures $T \sim 4\,\mathrm{MeV}$. In this paper, we have extended the virial equation of state of Refs. [11, 12] (for matter composed of neutrons, protons and alpha particles) to include ^{3}H and ^{3}He nuclei. We have made model-independent predictions for the abundance of ^{3}H and ^{3}He nuclei and predicted that their mass fractions can be significant near the neutrinosphere. Our results are directly based on nucleon-^{3}H and nucleon-^{3}He scattering phase shifts. In addition, it is interesting that ^{3}H nuclei can be more abundant than free protons at low temperatures, since many of the protons are bound in alpha particles (and heavy nuclei). In these regions, the rate of electron capture may be dominated by capture on ^{3}H nuclei [19].

While alpha particles are often more abundant, we have shown that the loosely-bound ^{3}H and ^{3}He nuclei dominate the energy transfer at low densities through inelastic excitations, and are therefore especially important for energy transfer from muon and tau neutrinos. Our new results for neutrino-^{3}H and -^{3}He neutral-current inclusive inelastic cross-sections and energy transfer cross-sections are based on microscopic two- and three-nucleon interactions and meson-exchange currents, which reproduce the triton half-life. All breakup channels and full final-state interactions were included via the LIT method. For temperatures $T \sim 4\,\mathrm{MeV}$, the predicted energy transfer cross-sections on mass-three nuclei are approximately one order of magnitude larger compared to inelastic excitations of ^{4}He nuclei.

Using the virial abundances and the microscopic energy tranfer cross-sections, we have found that mass-three nuclei contribute significantly to the neutrino energy loss due to inelastic excitations for $T \gtrsim 4\,\mathrm{MeV}$. Inelastic excitations of ^{3}H and ^{3}He nuclei can be more important than ^{4}He nuclei at high temperatures, low proton fraction or higher densities. To fully assess the role of neutrino breakup of $A = 3$ nuclei, our predicted abundances and neutral-current cross-sections should be included in SN simulations. The model independence of the virial equation of state and the accuracy of the predicted cross sections can help to improve the theoretical nuclear microphysics for SN simulations.

Acknowledgments

We thank Bill Donnelly for useful discussions and the Institute for Nuclear Theory, where some of this work was initiated, for its hospitality. This work was supported in part by the Natural Sciences and Engineering Research Council of Canada (NSERC), the US Department of Energy under Grant No. DE-FG02-87ER40365, and the ISRAEL SCIENCE FOUNDATION (Grant No. 361/05). TRIUMF receives federal funding via a contribution agreement through the National Research Council of Canada.

[1] R. Buras, H.-Th. Janka, M. Rampp and K. Kifonidis, astro-ph/0512189.

[2] H.-Th. Janka, K. Langanke, A. Marek, G. Martinez-Pinedo and B. Mueller, astro-ph/0612072.

[3] S.W. Bruenn, Astrophys. J. Suppl. **58** (1985) 771; A. Mezzacappa and S.W. Bruenn, Astrophys. J. **405** (1993) 637; **410** (1993) 740.

[4] W.C. Haxton, Phys. Rev. Lett. **60** (1988) 1999; S.W. Bruenn and W.C. Haxton, Astrophys. J. **3726** (1991) 678.

[5] S. Hannestad and G. Raffelt, Astrophys. J. **507** (1998) 339.

[6] A. Juodagalvis *et al.*, Nucl. Phys. **A747** (2005) 87.

[7] D. Gazit and N. Barnea, Phys. Rev. **C70** (2004) 048801.

[8] D. Gazit and N. Barnea, nucl-th/0701028.

[9] M.Th. Keil, G. Raffelt and H.-Th. Janka, Astrophys. J. **590** (2003) 971.

[10] N. Ohnishi, K. Kotake, and S. Yamada, Astrophys. J. **641** (2006) 1018.

[11] C.J. Horowitz and A. Schwenk, Nucl. Phys. **A776** (2006) 55.

[12] C.J. Horowitz and A. Schwenk, Phys. Lett. **B638** (2006) 153.

[13] M. Costantinit, A. Ianni and F. Visanni, Phys. Rev. **D70** (2004) 043006; C. Lunardini and A.Y. Smirnov, Astropart. Phys. **21** (2004) 703.

[14] S. Kowalski *et al.*, Phys. Rev. **C75** (2007) 014601.

[15] C.J. Horowitz and A. Schwenk, Phys.Lett. **B642** (2006) 326.

[16] V.D. Efros, W. Leidemann and G. Orlandini, Phys. Lett. **B238** (1994) 130.

[17] E. O'Connor, C.J. Horowitz and A. Schwenk, in prep.

[18] K. Huang, Statistical Mechanics, Wiley N.Y., Second Edition (1987), p. 224-227.

[19] E. O'Connor, D. Gazit, C.J. Horowitz, A. Schwenk and N. Barnea, in prep.

[20] R.B. Wiringa, V.G.J. Stoks and R. Schiavilla, Phys. Rev. **C51** (1995) 38.

[21] B.S. Pudliner, V.R. Pandharipande, J. Carlson, S.C. Pieper and R.B. Wiringa, Phys. Rev. **C56** (1997) 1720.

[22] N. Barnea, W. Leidemann and G. Orlandini, Phys. Rev. **C61** (2000) 054001; Nucl. Phys. **A693** (2001) 565.

[23] N. Barnea and A. Novoselsky, Ann. Phys. (N.Y) **256** (1997) 192.

[24] V.D. Efros, W. Leidemann, G. Orlandini and E.L. Tomusiak, Phys. Rev. **C69** (2004) 044001.

[25] D. Gazit, S. Bacca, N. Barnea, W. Leidemann and G. Orlandini, Phys. Rev. Lett. **96** (2006) 112301.

[26] T.-S. Park *et al.*, Phys. Rev. **C67** (2003) 055206.